Supporting Information for:

Chromophore Orientation-Dependent Photophysical Properties of Pyrene-Naphthalimide Compact Electron Donor-Acceptor Dyads: Electron Transfer and Intersystem Crossing

Muhammad Imran,[a] Andrey A. Sukhanov,[b] Partha Maity,[c] Ayhan Elmali,[d] Jianzhang Zhao,*[,a] Ahmet Karatay,*[,d] Omar F. Mohammed*[,c] and Violeta K. Voronkova*[,b]

[a] State Key Laboratory of Fine Chemicals, School of Chemical Engineering, Dalian University of Technology, E–208 West Campus, 2 Ling Gong Rd., Dalian 116024, P. R. China. E–mail: zhaojzh@dlut.edu.cn

[b] Zavoisky Physical-Technical Institute, FRC Kazan Scientific Center of RAS, Kazan 420029, Russia. E-mail: vio@kfti.knc.ru

[c] Division of Physical Sciences and Engineering, King Abdullah University of Science and Technology (KAUST), Thuwal 23955-6900, Kingdom of Saudi Arabia. E-mail: omar.abdelsaboor@kaust.edu.sa

[d] Department of Engineering Physics, Faculty of Engineering, Ankara University, 06100 Beşevler, Ankara, Turkey. E-mail: ahmet.karatay@eng.ankara.edu.tr

Index

1. Synthesis of reference compounds……Page S3
2. NMR and HRMS spectra……Page S5
3. UV−vis absorption and fluorescence emission spectra……Page S13
4. Phosphorescence spectra……Page S14
5. Room temperature fluorescence lifetime spectra……Page S14
6. Temperature-dependent fluorescence lifetime spectra……Page S15
7. Measurement of singlet oxygen quantum yield……Page S16
8. Electrochemical and spectroelectrochemical study……Page S17
9. Nanosecond transient absorption spectroscopy……Page S19
10. Intrinsic triplet state lifetime fitting procedure……Page S23
11. Femtosecond transient absorption spectroscopy……Page S25
12. Computational study……Page S28
13. x,y,z coordinates of the optimized geometries……Page S30
14. References……Page S35

1. Synthesis of Reference Compounds

Synthesis of NI-3Br. Under N_2 atmosphere, 3-bromo-1,8-naphthalic anhydride (554.1 mg, 2.0 mmol), *n*-butylamine (146 mg, 2.0 mmol) and ethanol (20 mL) were mixed together. The reaction mixture was refluxed at 78 °C for 5 h. On completion of reaction, solvent was removed under reduced pressure and the crude product was purified by column chromatography (silica gel, DCM/ *n*-hexane = 1:1.5, v/v) to give white solid (400 mg, yield: 60%). ^{1}H NMR ($CDCl_3$, 400 MHz): δ 8.67 (d, 1H, J = 8.0 Hz), 8.62 (d, 1H, J = 8.0 Hz), 8.38 (d, 1H, J = 8.0 Hz), 8.15 (d, 1H, J = 8.0 Hz), 7.79 (t, 1H, J = 8.0 Hz), 4.20 (t, 2H, J = 8.0 Hz), 1.77 – 1.69 (m, 2H), 1.50 – 1.44 (m, 2H), 1.0 (t, 3H, J = 8.0 Hz). MALDI-TOF-HRMS: Calcd ($[C_{16}H_{15}BrNO_2]^+$), m/z = 332.0286; found, m/z = 332.0284.

Synthesis of NI-4Br. Compound **NI-4Br** was synthesized with a method similar to that of **NI-3Br.** The product was obtained as white solid (yield: 62 %). ^{1}H NMR ($CDCl_3$, 400 MHz): δ 8.66 (d, 1H, J = 8.0 Hz), 8.56 (d, 1H, J = 8.0 Hz), 8.41 (d, 1H, J = 8.0 Hz), 8.04 (d, 1H, J = 8.0 Hz), 7.84 (t, 1H, J = 8.0 Hz), 4.17 (t, 2H, J = 8.0 Hz), 1.75 – 1.68 (m, 2H), 1.48 – 1.42 (m, 2H), 0.98 (t, 3H, J = 8.0 Hz). TOF MS EI+: Calcd ($[C_{16}H_{14}BrNO_2]^+$), m/z = 331.0208; found, m/z = 331.0213.

Synthesis of NI-3Ph. Under N_2 atmosphere, **NI-3Br** (265.7 mg, 0.8 mmol), phenylboronic acid (97.5 mg, 0.8 mmol), K_2CO_3 (330 mg, 2.3 mmol) and EtOH/toluene/H_2O (v/v/v = 2: 2:1, 50 mL) were mixed together. After N_2 bubbling for 20 minutes, $Pd(pph_3)_4$ (20.2 mg, 0.039 mmol) was added and refluxed at 90 °C for 10 h. After completion of the reaction, the mixture was cooled to room temperature and extracted with DCM (3 × 20 mL). The organic layer was

washed with H_2O and dried over anhydrous Na_2SO_4. Solvent was removed under reduced pressure and crude product was purified by column chromatography (silica gel, DCM/*n*-hexane = 1:4, v/v) to give white solid (150 mg, yield: 57%). Mp: 147.0 – 148.0 °C. ^{1}H NMR ($CDCl_3$, 400 MHz): δ = 8.88 (s, 1H), 8.60 (d, 1H, *J* = 8.0 Hz), 8.39 (s, 1H), 8.27 (d, 1H, *J* = 8.0 Hz), 7.80 (d, 3H, *J* = 8.0 Hz), 7.57 – 7.47 (m,3H), 4.23 (t, 2H, *J* = 8.0 Hz), 1.80 – 1.72 (m, 2H), 1.54 – 1.44 (m, 2H), 1.01 (t, 3H, *J* = 8.0 Hz). MALDI-TOF-HRMS: Calcd ($[C_{22}H_{20}NO_2]^+$), *m/z* = 330.1494; found, *m/z* = 330.1501.

Synthesis of NI-4Ph. Compound **NI-4Ph** was synthesized with a method similar to that of **NI-3Ph.** The product was obtained as white solid (yield: 57 %). Mp: 147.0 – 148.0 °C. ^{1}H NMR ($CDCl_3$, 400 MHz): δ = 8.66 (d, 2H, *J* = 8.0 Hz), 8.29 (d, 1H, *J* = 8.0 Hz), 7.72 (d, 2H, *J* = 8.0 Hz), 7.60 – 7.52 (m, 5H), 4.26 (t, 2H, *J* = 8.0 Hz), 1.81 – 1.73 (m, 2H), 1.54 – 1.45 (m, 2H), 1.02 (t, 3H, *J* = 8.0 Hz). TOF MS EI$^+$: Calcd ($[C_{22}H_{19}NO_2]^+$), *m/z* = 329.1416; found, *m/z* = 329.1420.

2. NMR and HRMS Spectra of Compounds

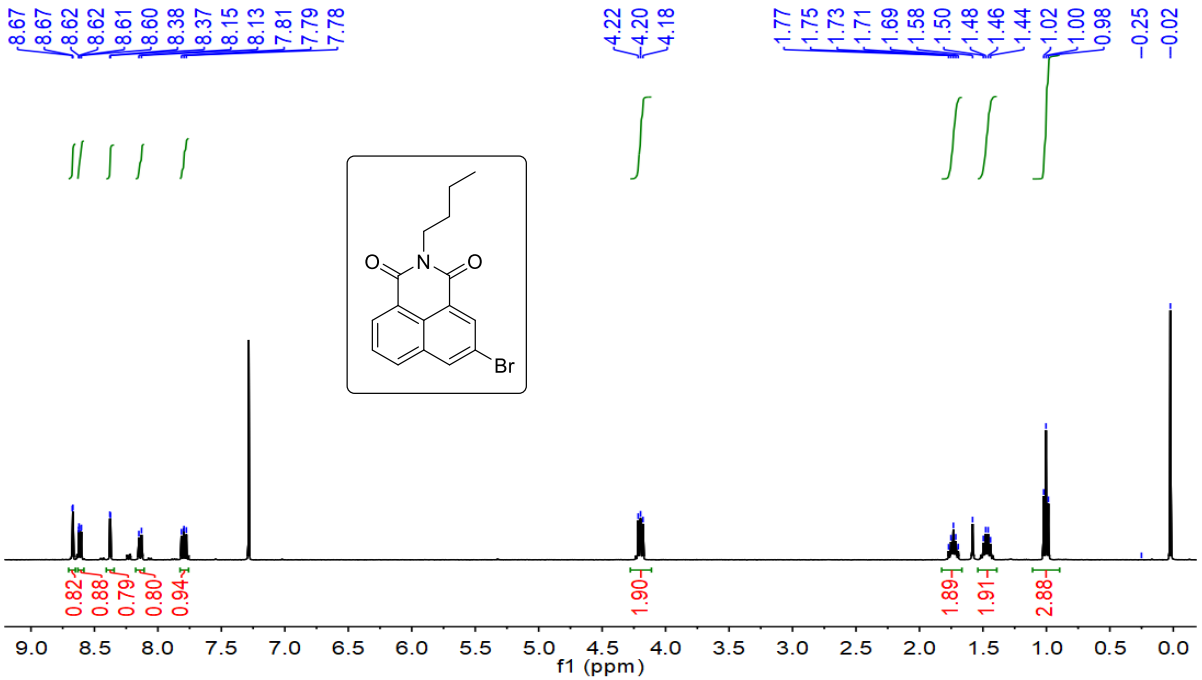

Figure S1. ^{1}H NMR spectrum of compound **NI-3Br** in $CDCl_3$ (400 MHz), 25 °C.

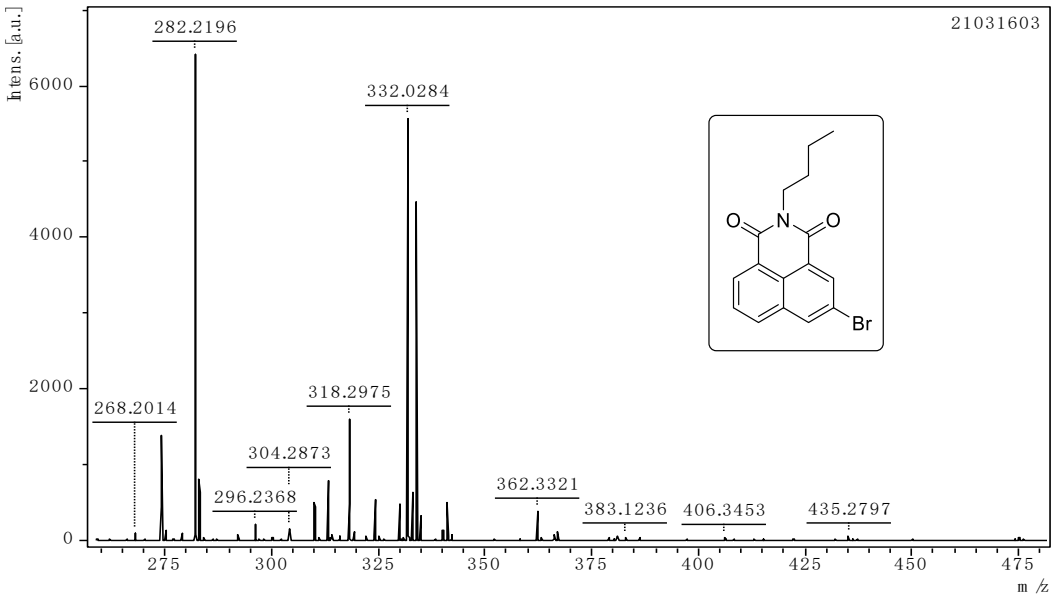

Figure S2. MALDI-TOF-HRMS spectrum of compound **NI-3Br**.

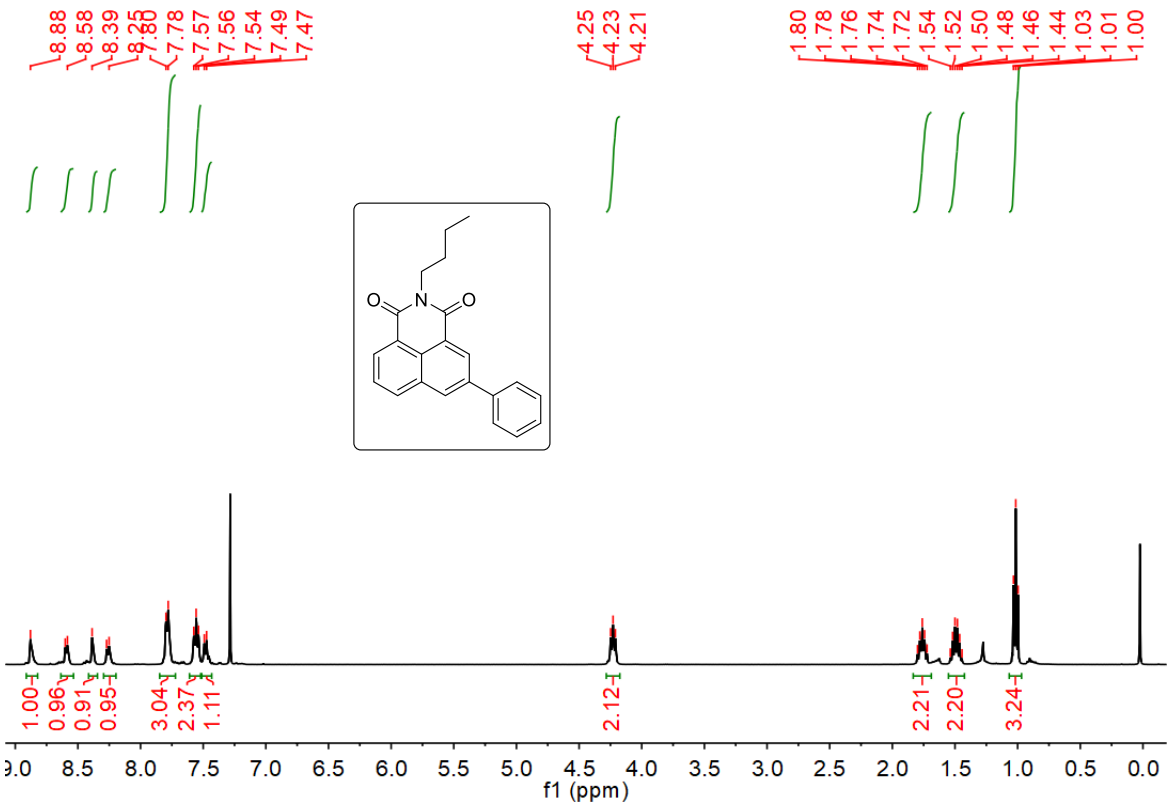

Figure S3. ^{1}H NMR spectrum of compound **NI-3Ph** in $CDCl_3$ (400 MHz), 25 °C.

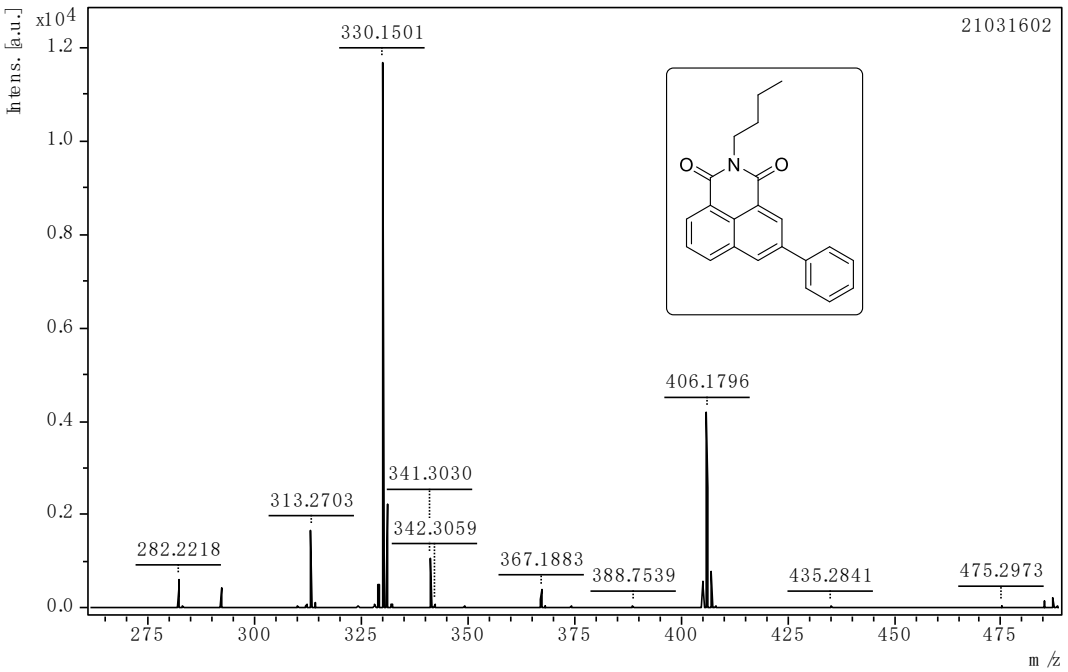

Figure S4. MALDI-TOF-HRMS spectrum of compound **NI-3Ph**.

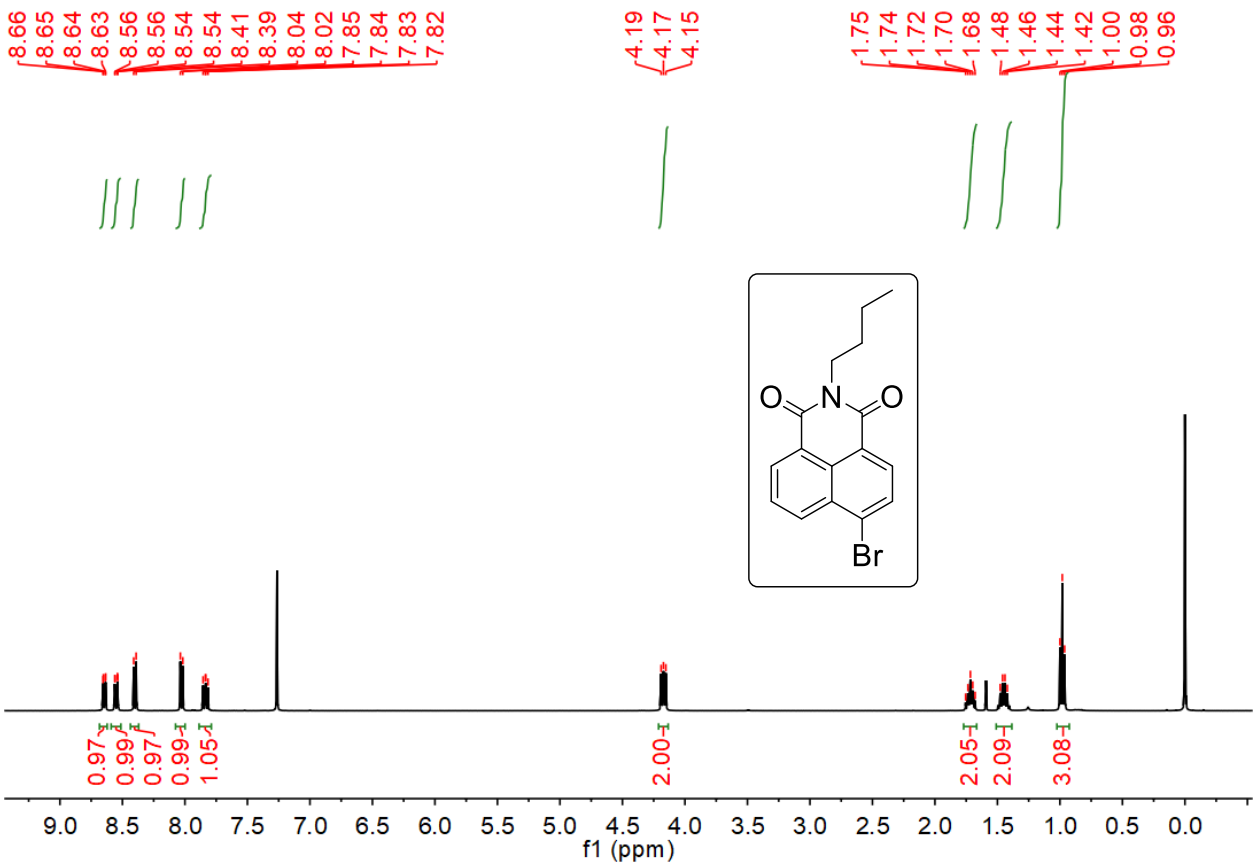

Figure S5. ^{1}H NMR spectrum of compound **NI-4Br** in $CDCl_3$ (400 MHz), 25 °C.

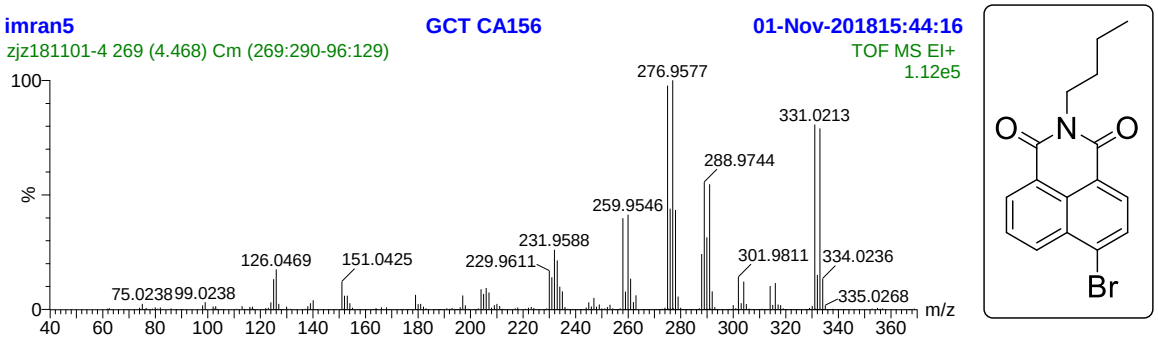

Figure S6. TOF-MS EI^{+} spectrum of compound **NI-4Br**.

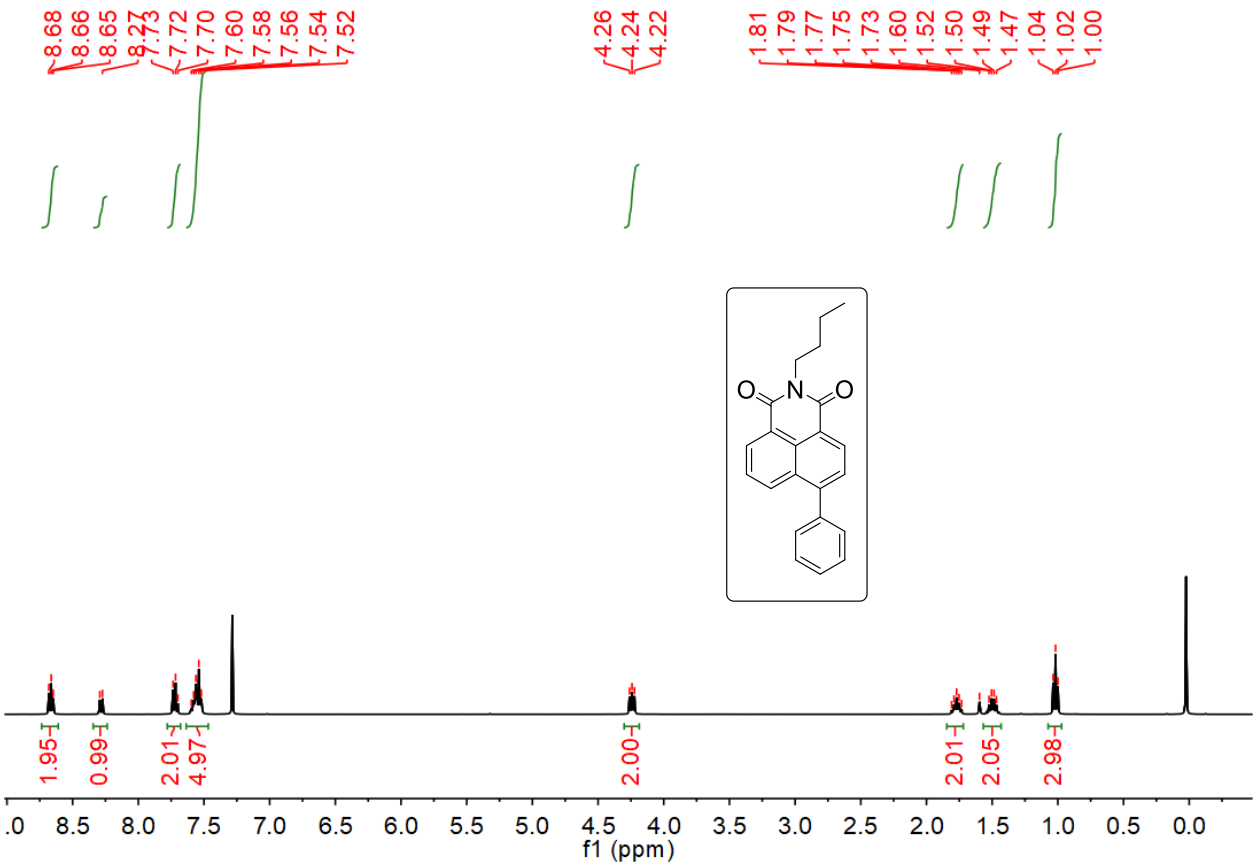

Figure S7. ^{1}H NMR spectrum of compound **NI-4Ph** in $CDCl_3$ (400 MHz), 25 °C.

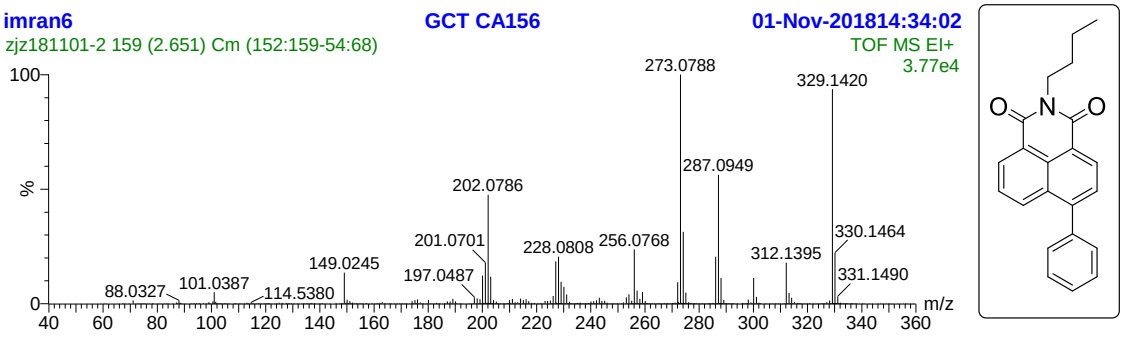

Figure S8. TOF-MS EI^{+} spectrum of **NI-4Ph**.

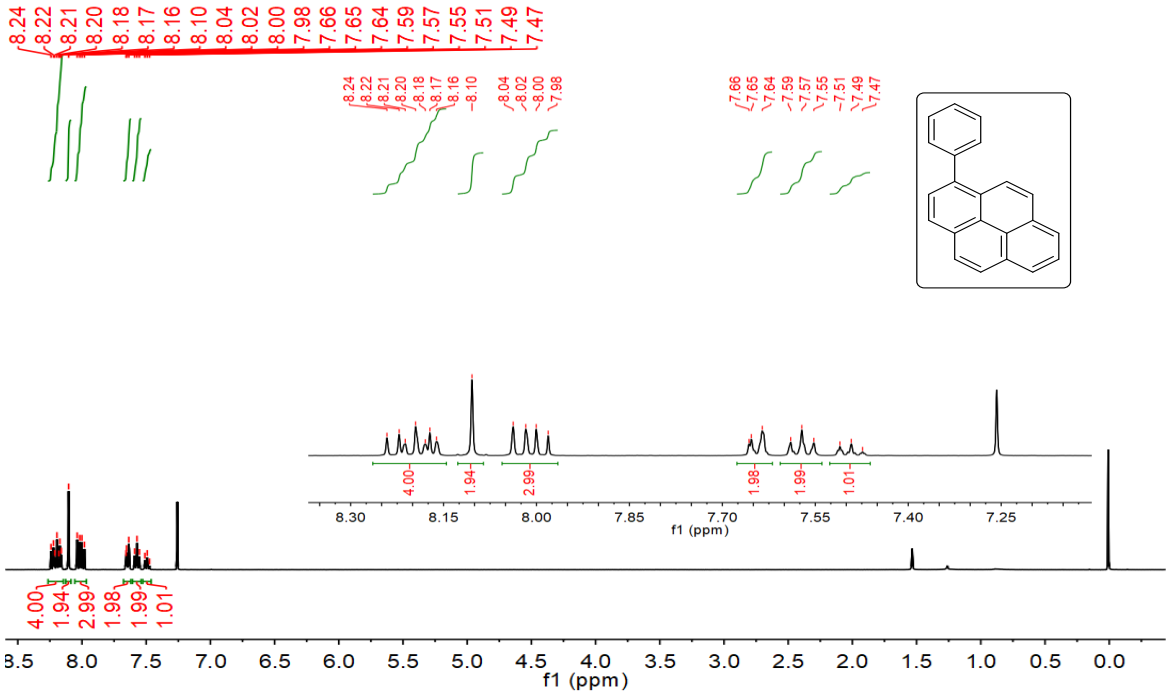

Figure S9. ^{1}H NMR spectrum of compound **Py-Ph** in $CDCl_3$ (400 MHz), 25 °C.

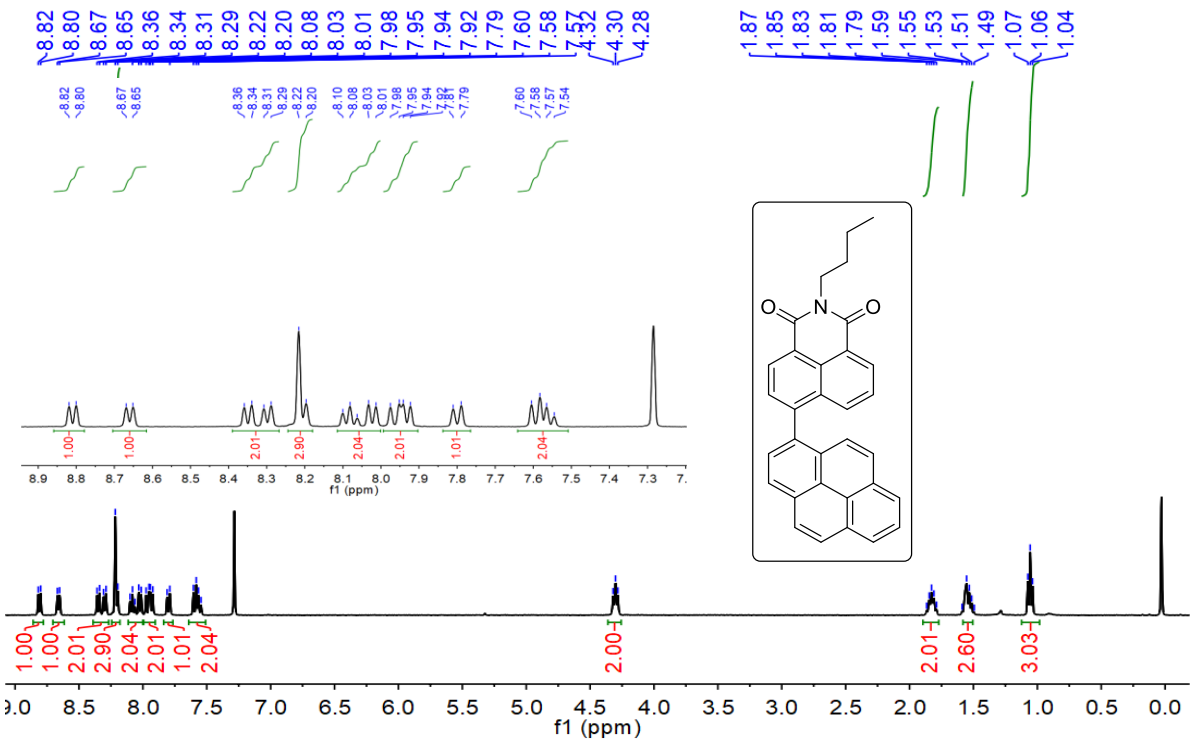

Figure S10. ^{1}H NMR spectrum of compound **NI-Py-1** in $CDCl_3$ (400 MHz), 25 °C.

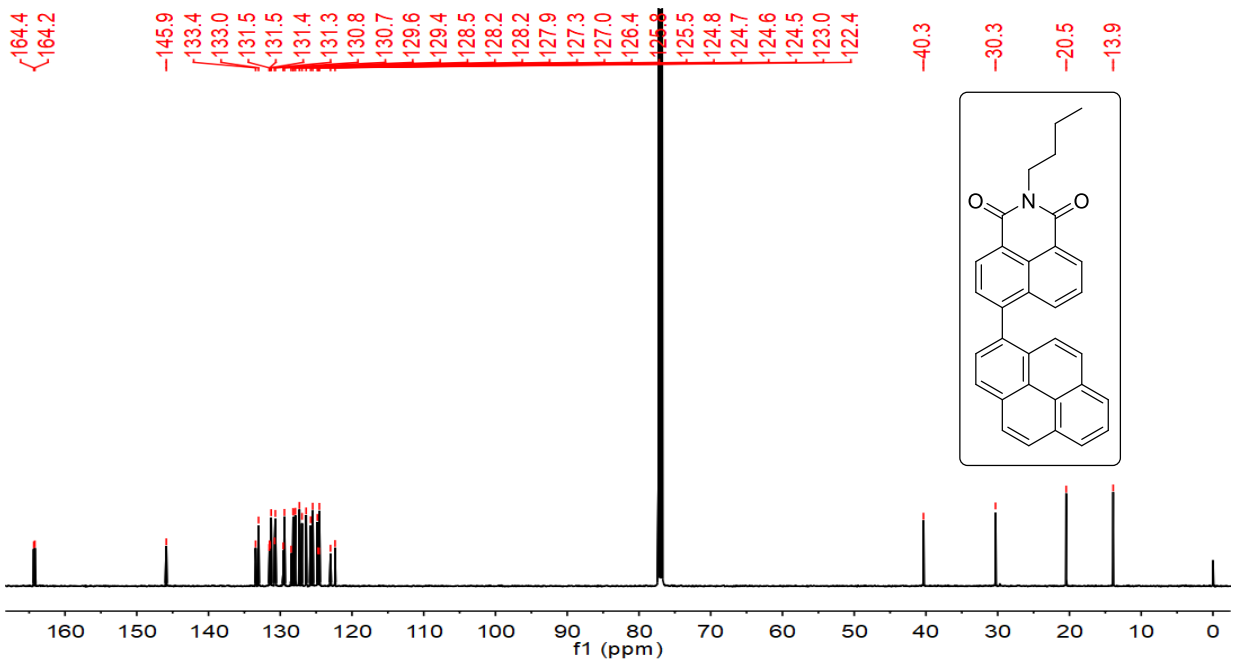

Figure S11. ^{13}C NMR spectrum of compound **NI-Py-1** in $CDCl_3$ (126 MHz), 25 °C.

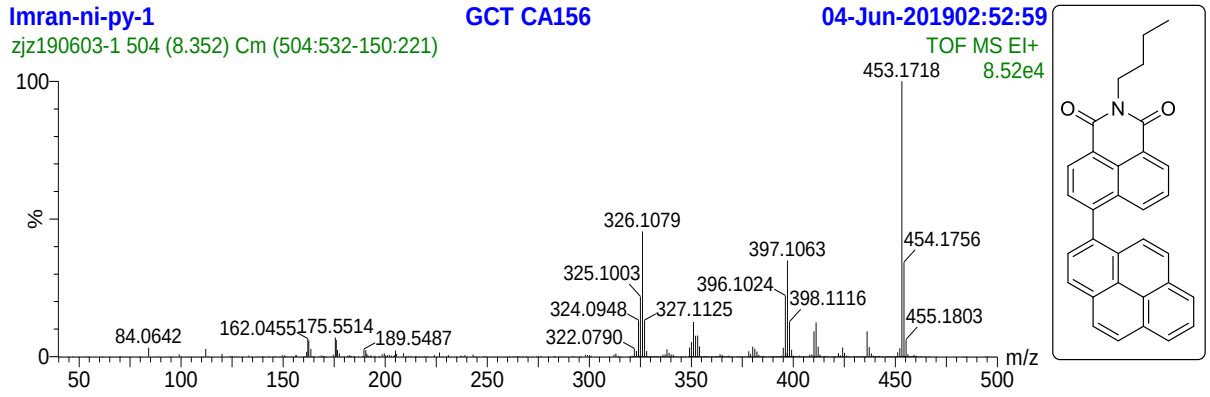

Figure S12. TOF-MS EI^+ spectrum of **NI-Py-1**.

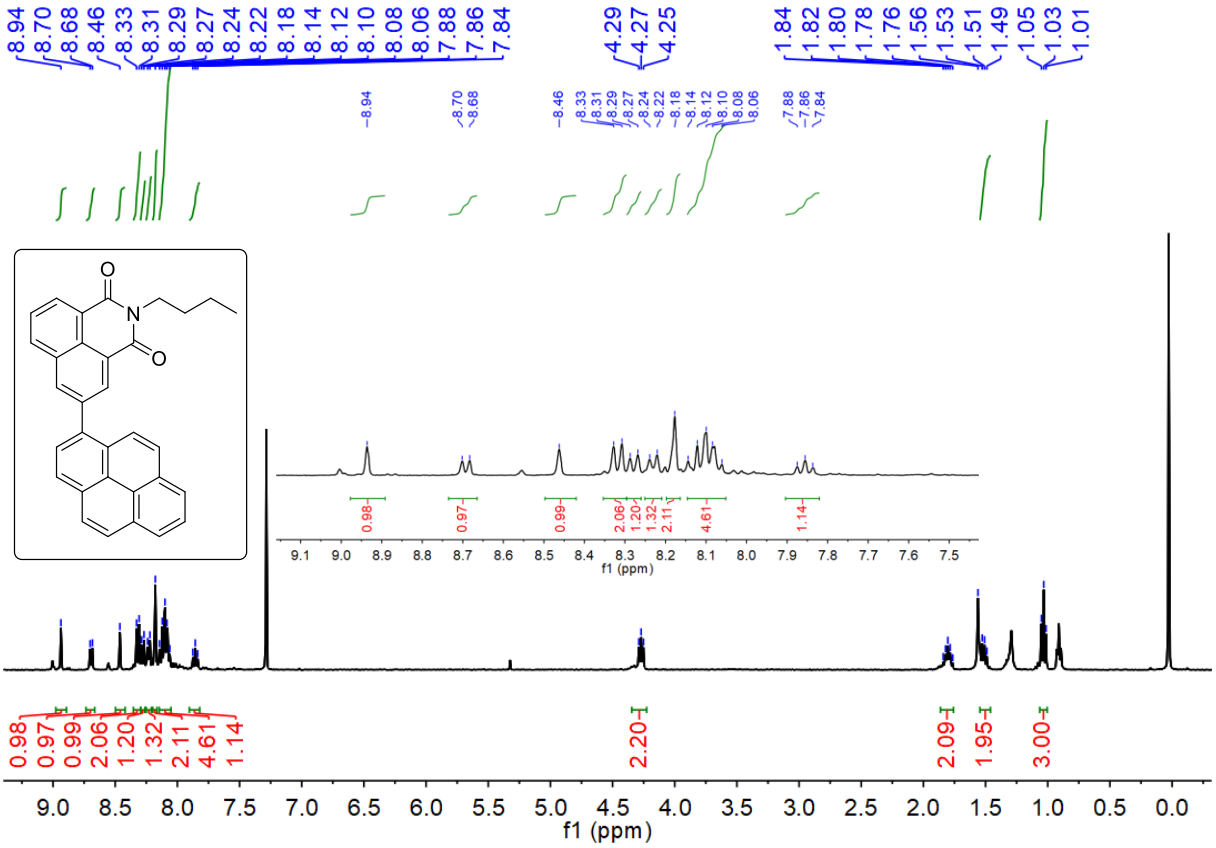

Figure S13. ^{1}H NMR spectrum of compound **NI-Py-2** in $CDCl_3$ (400 MHz), 25 °C.

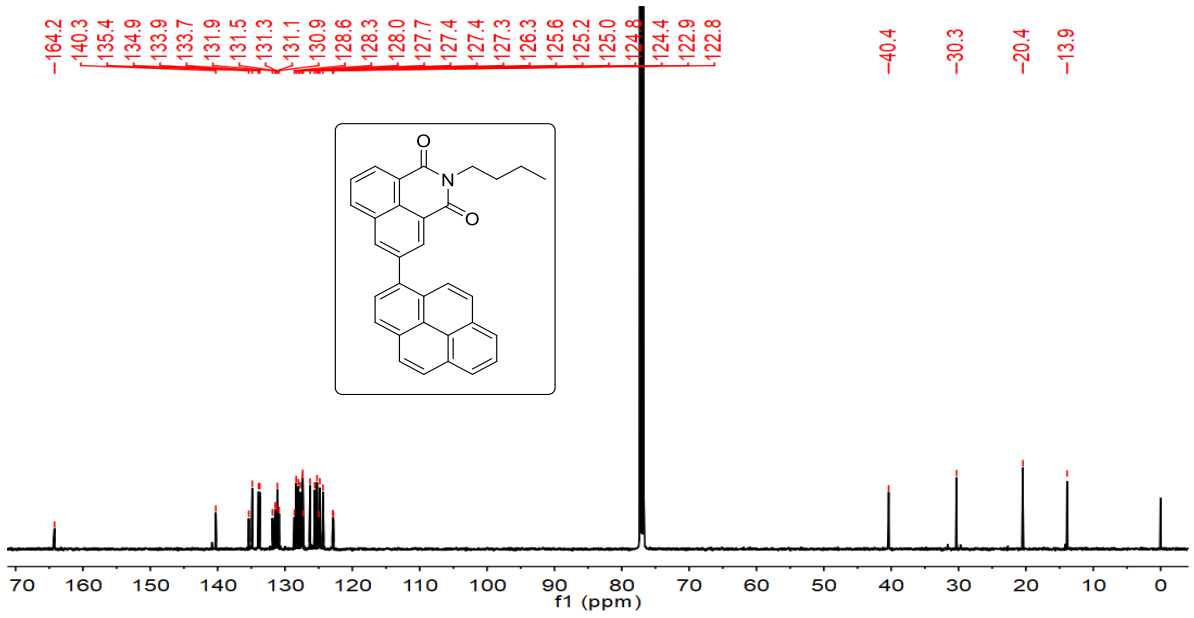

Figure S14. ^{13}C NMR spectrum of compound **NI-Py-2** in $CDCl_3$ (126 MHz), 25 °C.

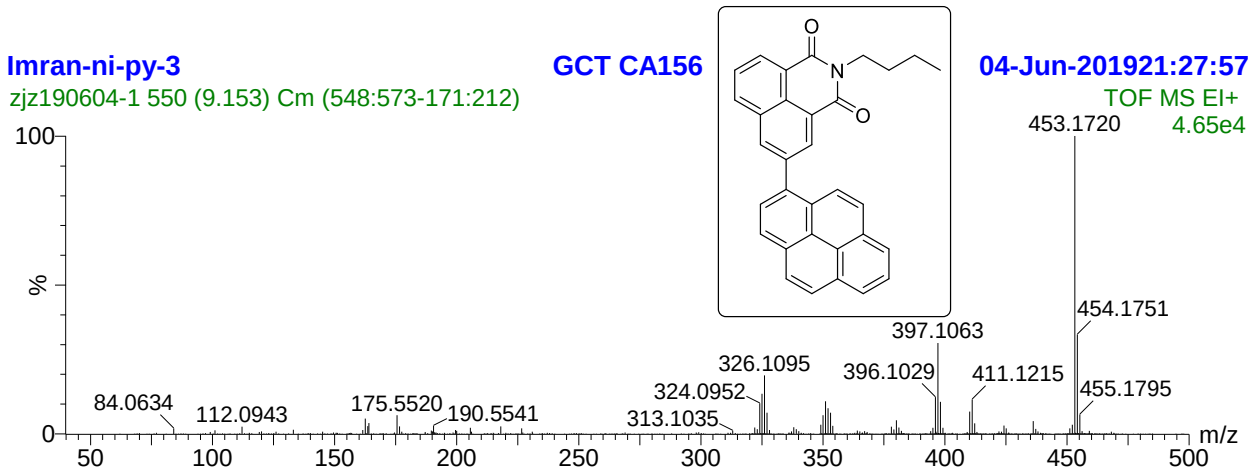

Figure S15. TOF-MS EI⁺ spectrum of **NI-Py-2**.

3. UV–vis absorption and fluorescence emission spectra

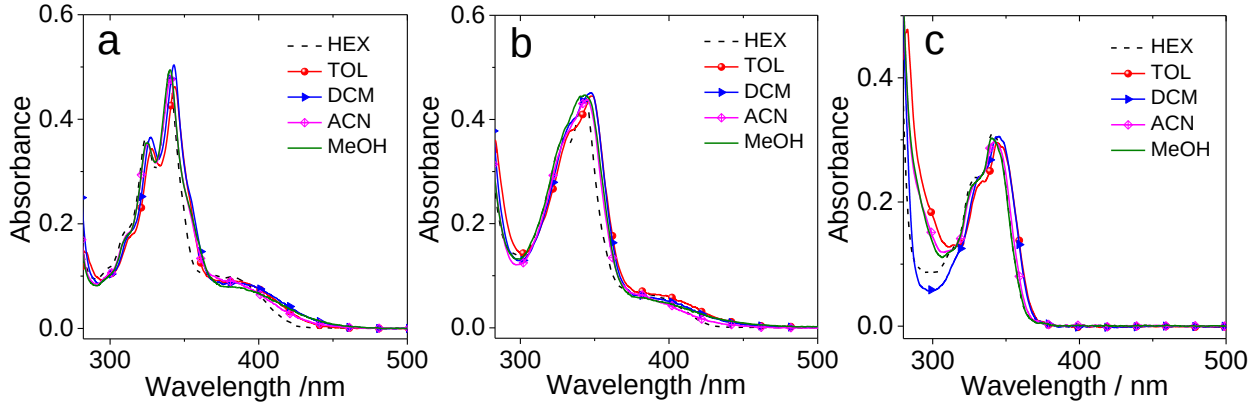

Figure 16. UV−vis absorption spectra of (a) **NI-Py-1**, (b) **NI-Py-2** and (c) **Py-Ph** in different solvents, c = 1.0 × 10^{-5} M, 20 °C.

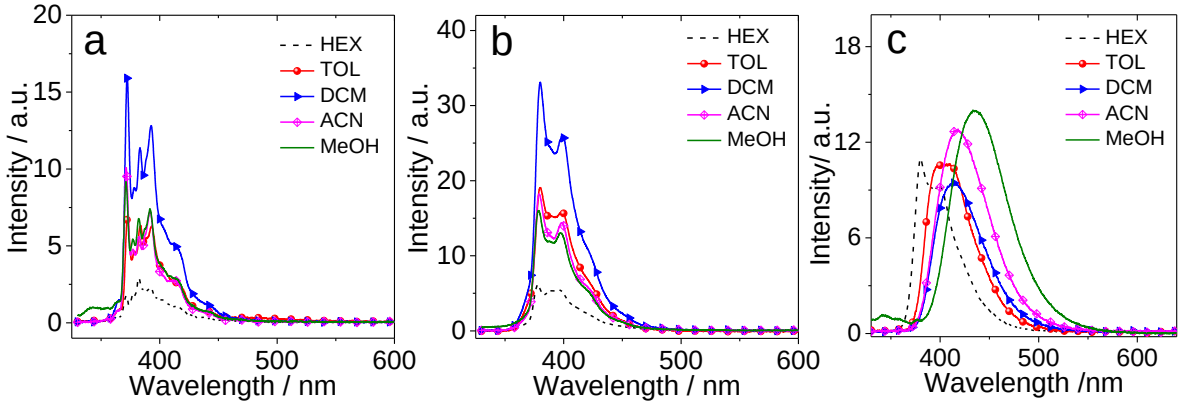

Figure S17. Fluorescence emission spectra of (a) **Py**, (b) **Py-Ph** and (c) **NI-3Ph** in different solvents. Excited with a picosecond pulsed laser (340 nm). c = 1.0 × 10^{-5} M. 20 °C.

4. Phosphorescence spectra

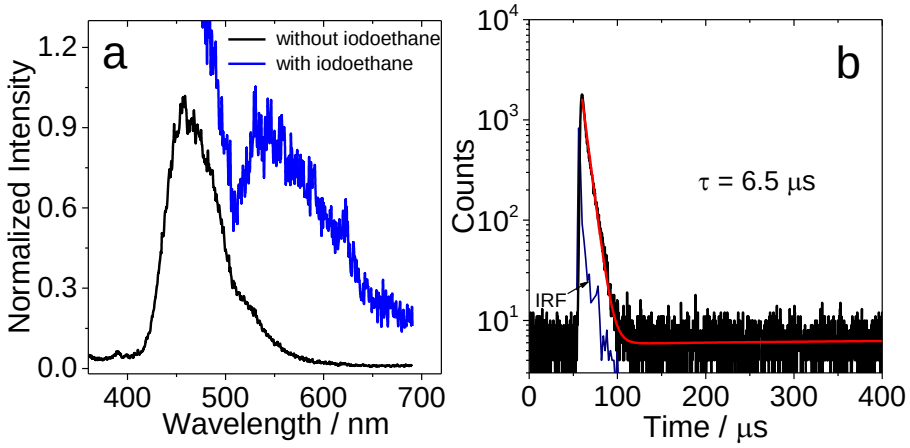

Figure S18. Normalized phosphorescence emission spectra of **NI-Py-2** (with and without 20 % ethyl iodide) at 77 K in frozen THF. (b) Phosphorescence decay in the presence of 20 % iodoethane. $c = 3.0 \times 10^{-5}$ M. Measurements were carried out with excitation using μF920 lamp at 350 nm.

5. Room temperature fluorescence lifetime spectra

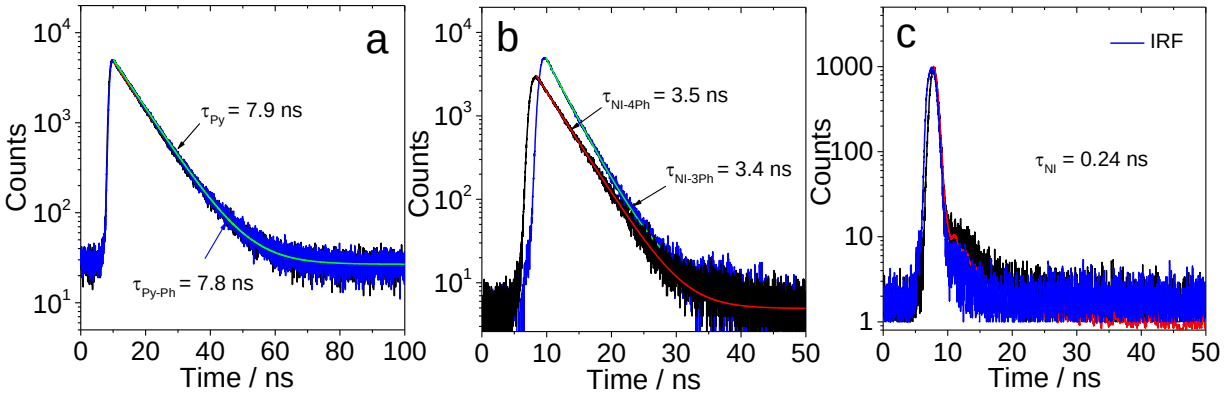

Figure S19. (a) Fluorescence lifetime decay curves of Py and **Py-Ph** at 380 nm In *n*-hexane. (b) Fluorescence lifetime decay curves of **NI-3Ph** and **NI-4Ph** in DCM. (c) Fluorescence lifetime decay curve of pristine **NI** in DCM. Excited with picosecond pulsed laser (340 nm). $c = 1.0 \times 10^{-5}$. M. 20 °C.

6. Temperature-dependent fluorescence

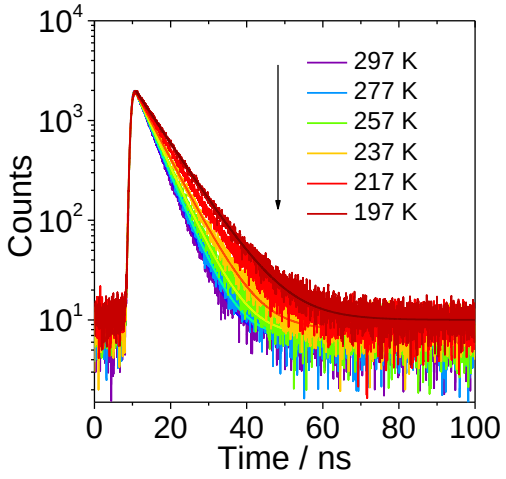

Figure S20. Temperature-dependent fluorescence lifetime curves of **NI-Py-1** at 550 nm. Excited with a picosecond pulsed laser (340 nm). $c = 1.0 \times 10^{-5}$ M.

7. Measurement of singlet oxygen quantum yield

Singlet oxygen quantum yields of the compounds (mentioned in Table 2) were measured with anthracene as standard (Φ_Δ = 0.70 in MeOH). 1,3-Diphenylisobenzofuran (DPBF) was used as $^1O_2$ scavenging agent. The absorbance of DBBF was adjusted to around 1.0 in the air saturated dichloromethane (DCM) solvent. After that, compound was added to the solution of DPBF, and the compound's absorbance was adjusted between 0.2−0.3. A monochromatic light was used to irradiate the solution in the cuvette for 30 seconds at the wavelength of peak absorption. Then the absorbance at 414 nm was measured after each irradiation and took 10 readings continuously. The slope of the plots of the absorbance of DPBF at 414 nm vs irradiation time for each compound was calculated. Singlet oxygen quantum yields were calculated by using the following equation S1:

$$\Phi_{\Delta,sam} = \Phi_{\Delta,std}\left(\frac{1-10^{-A_{std}}}{1-10^{-A_{sam}}}\right)\left(\frac{m_{sam}}{m_{std}}\right)\left(\frac{\eta_{sam}}{\eta_{std}}\right)^2 \qquad \text{(S1)}$$

Where '*sam*' and '*std*' designate the compounds and standard anthracene respectively, *A* stands for absorbance, *m* is the slope of the curves of absorbance of DPBF at 414 nm versus the irradiation time, η is the refractive index of the solvent.

8. Electrochemical and spectroelectrochemical study

Gibbs free energy changes of photo-induced electron transfer process were calculated using Weller equation S2 and S3.[1–3] The calculation indicates that the charge separation (electron transfer) is thermodynamically allowed even in non-polar solvents and more favorable in polar solvents, which is in agreement with the fluorescence studies.

$$\Delta G^{0}_{\mathrm{CS}} = e[E_{OX} - E_{RED}] - E_{00} + \Delta G_{\mathrm{S}} \qquad \text{(S2)}$$

$$\Delta G_{\mathrm{S}} = -\frac{e^2}{4\pi\varepsilon_{\mathrm{s}}\varepsilon_0 R_{CC}} - \frac{e^2}{8\pi\varepsilon_0}\left(\frac{1}{R_{\mathrm{D}}} + \frac{1}{R_{\mathrm{A}}}\right)\left(\frac{1}{\varepsilon_{REF}} - \frac{1}{\varepsilon_{\mathrm{S}}}\right) \qquad \text{(S3)}$$

Here ΔG_{CS} is the static Columbic energy, which is described by equation 1. In eq. 1 and 2, e = electronic charge, E_{OX} = half-wave potential of the electron-donor unit for one-electron oxidation, E_{RED} = half-wave potential of the electron-acceptor unit for one-electron reduction; E_{00} = approximated energy level with the cross point of normalized UV–vis absorption and fluorescence emission spectra at singlet excited state of pyrene moiety, ε_{S} = static dielectric constant of the solvent, R_{CC} = center-to-center distance between pyrene (electron donor unit) and naphthalimide (electron acceptor unit) determined by DFT optimization of the geometry, R_{CC} [(**NI-Py-1**) = 7.318 Å] and R_{CC} [(**NI-Py-2**) = 7.687 Å], R_{D}, is the radius of the electron donor, R_{A}, is the radius of the electron acceptor, $\varepsilon_{\mathrm{REF}}$ is the static dielectric constant of the solvent used for the electrochemical studies, ε_0 is the permittivity of free space. The following solvents were used in the calculation of the free energy of electron transfer, toluene (ε_{S} = 2.38), DCM (ε_{S} = 9.1), and ACN (ε_{S} = 37.5).

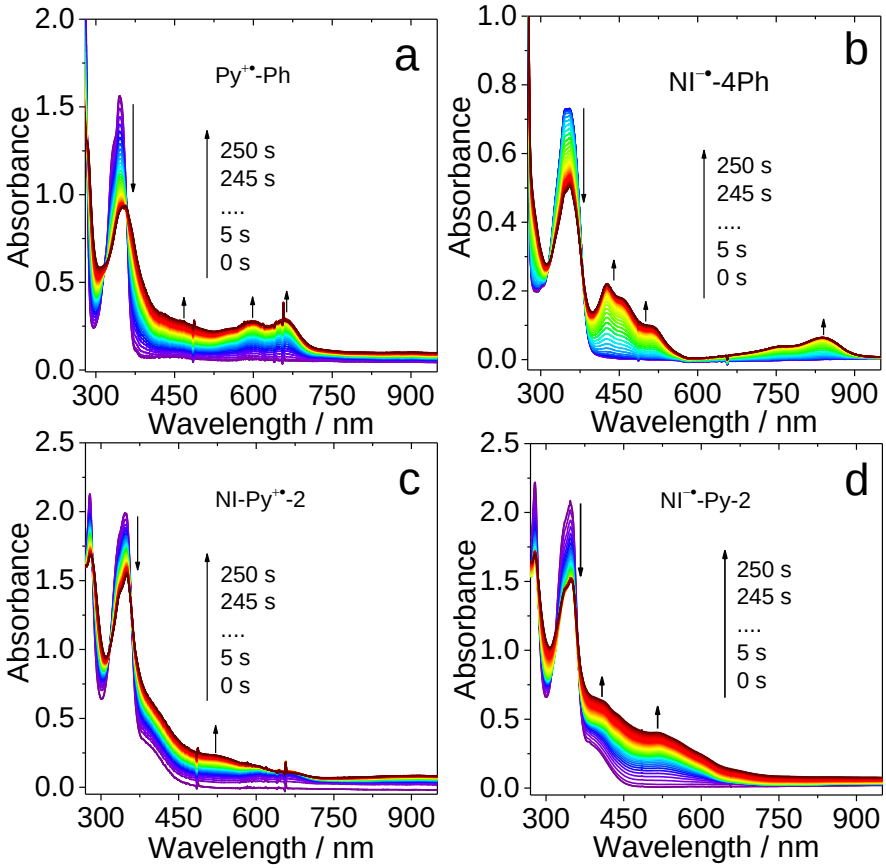

Figure S21. UV–vis absorption spectral changes of compounds measured with spectroelectrochemical method, (a) upon oxidation of **Py-Ph** under 1.17 eV, (b) upon reduction of **NI-4Ph** under – 1.70 eV, (c) upon oxidation of **NI-Py-2** under 1.17 eV and (d) upon reduction of **NI-Py-2** under – 1.70 eV. All the experiments were carried out in deaerated DCM containing $Bu_4N[PF_6]$ (ca. 0.1M) as supporting electrolytes, $Ag/AgNO_3$ as the reference electrode. Ferrocene (Fc) was used as an internal reference. Scan rates: 50 mV/s. $c = 1.0 \times 10^{-3}$ M. 20 °C.

9. Nanosecond transient absorption spectroscopy

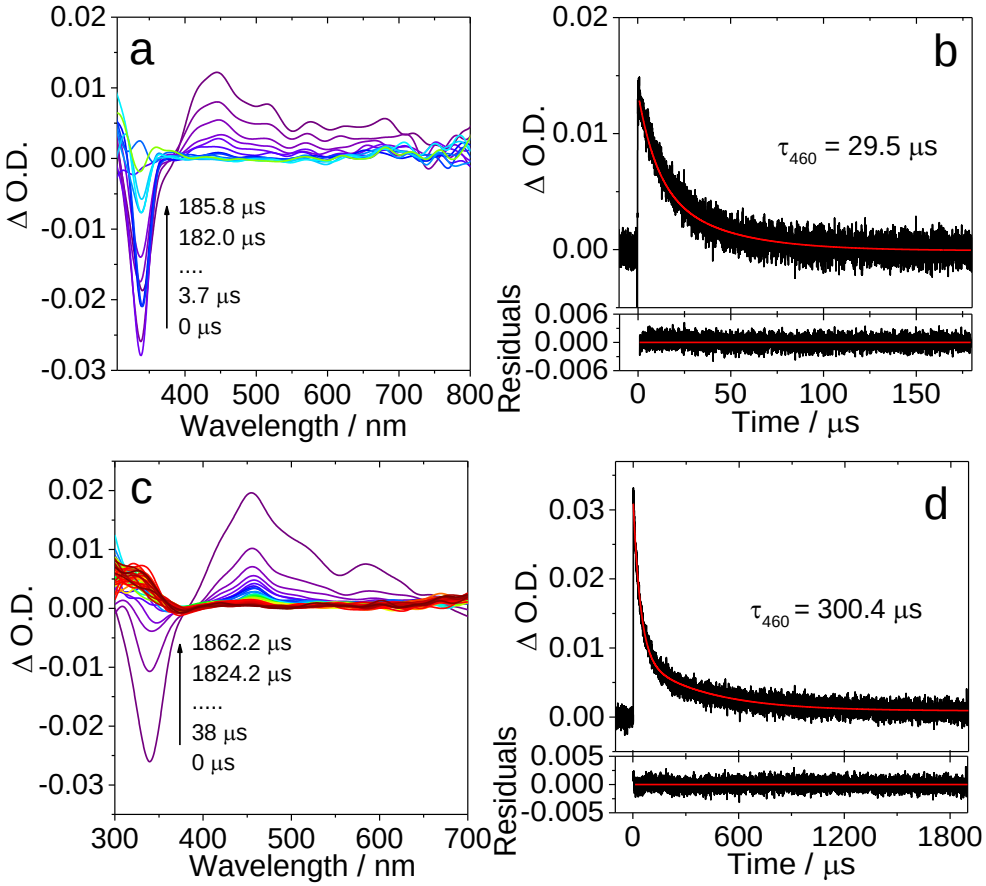

Figure S22. Nanosecond transient absorption spectra of **NI-Py-1** (a) in deaerated *n*-hexane (b) respective decay trace at 460 nm, c = 2.0 ×10^{-5} M, (c) in deaerated ACN (d) respective decay trace at 470 nm, c = 1.0 ×10^{-5} M. λ_{ex} = 355 nm. 20 °C.

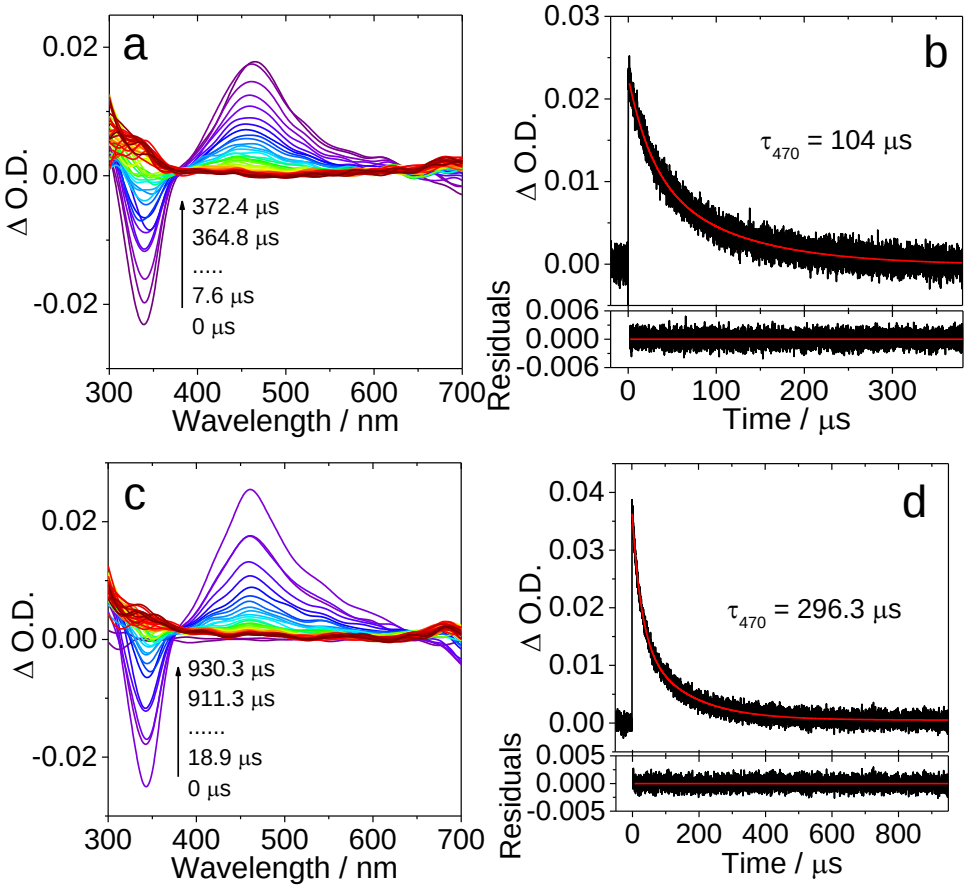

Figure S23. Nanosecond transient absorption spectra of **NI-Py-2** (a) in deaerated *n*-hexane (b) respective decay trace at 470 nm, c = 5.0 ×10^{-5} M, (c) in deaerated ACN (d) respective decay trace at 470 nm, c = 1.0 ×10^{-5} M. λ_{ex} = 355 nm. 20 °C.

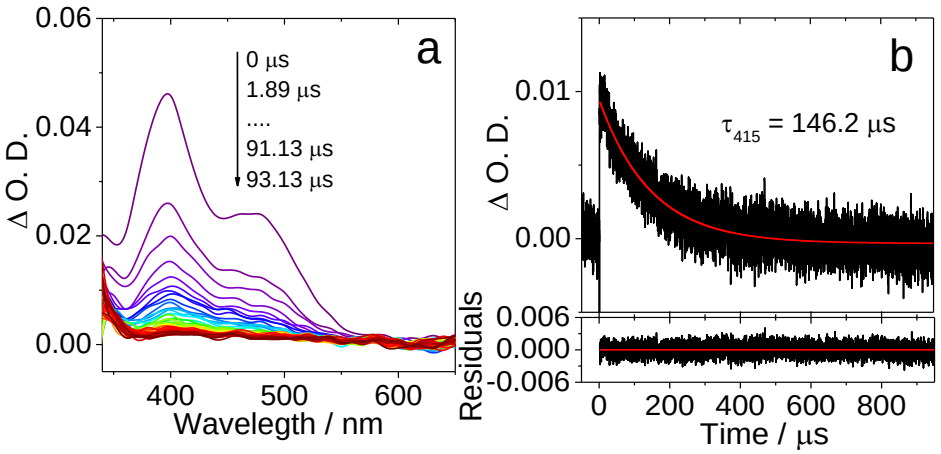

Figure S24. Nanosecond transient absorption spectra of (a) **Pyrene,** in deaerated toluene with 30% iodoethane, λ_{ex} = 330 nm; (b) respective decay trace at 415 nm without iodoethane. c = 2.0 × 10^{-5} M. 20 °C.

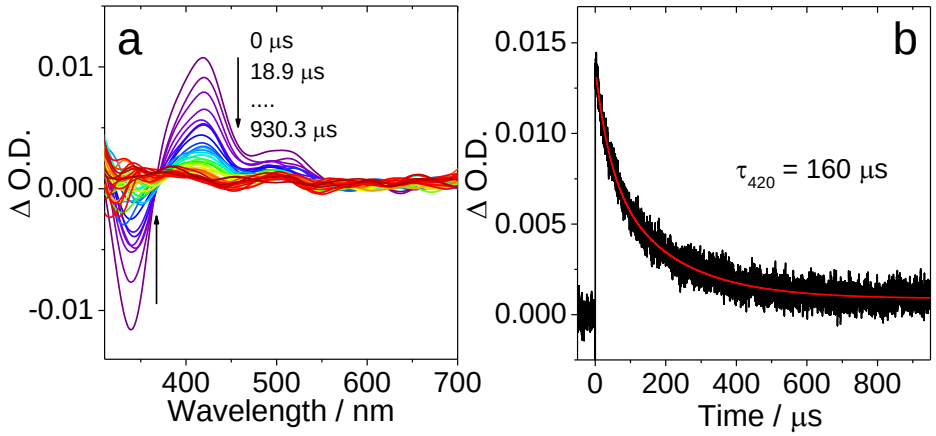

Figure S25. (a) Nanosecond transient absorption spectra of **Py-Br,** (b) decay trace at 420 nm. λ_{ex} = 345 nm. c = 2.0 × 10^{-5} M. In deaerated toluene. 20 °C.

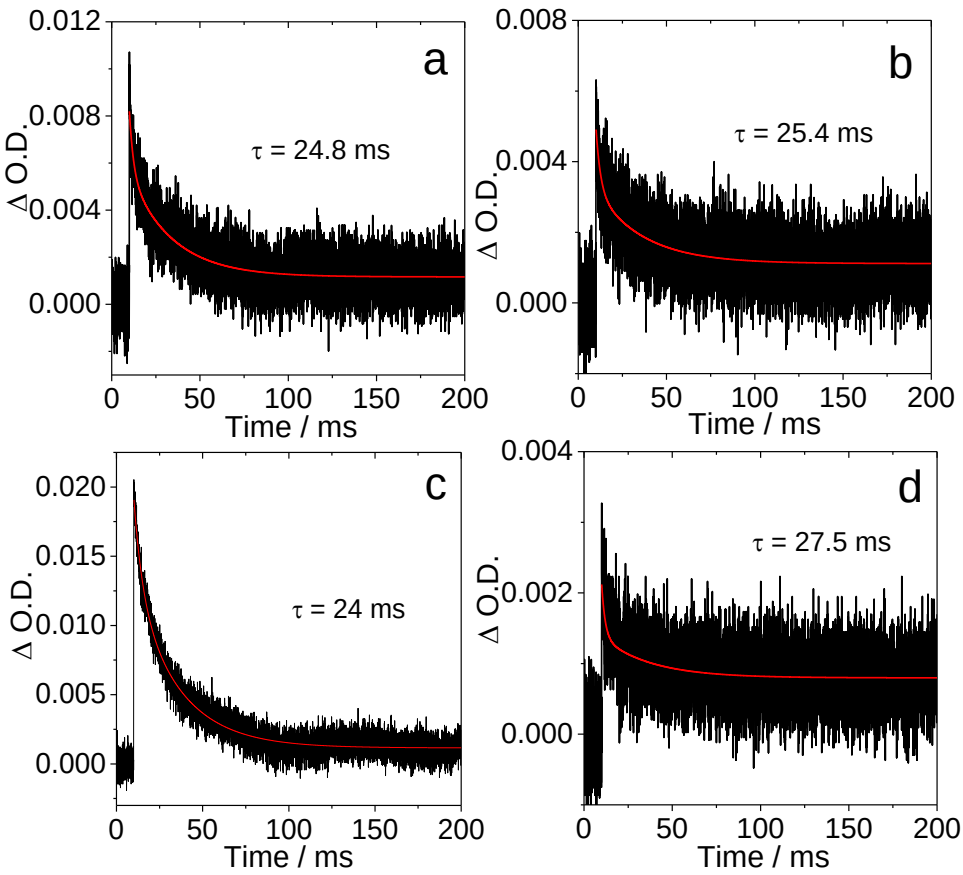

Figure S26. Nanosecond transient absorption decay traces at 460 nm of **NI-Py-1** (a) in (Clear Flex 50®) (b) polymethylmethacrylate (PMMA). Nanosecond transient absorption decay traces at 470 nm of **NI-Py-2** (c) in (Clear Flex 50®) (d) polymethylmethacrylate (PMMA). λ_{ex} = 355 nm. 20 °C.

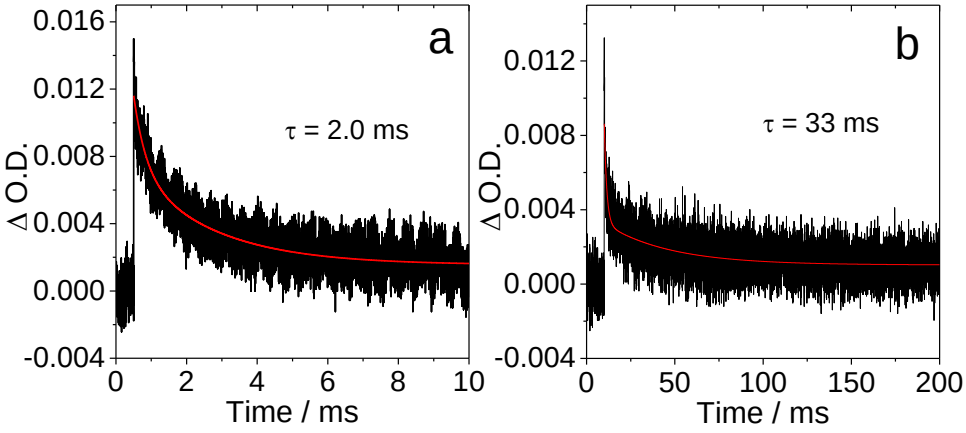

Figure S27. Nanosecond transient absorption decay trace of (a) **Py-Br** at 450 nm and (b) **NI-4Ph** at 540 nm. In polymethylmethacrylate (PMMA). λ_{ex} = 355 nm. 20 °C.

10. Intrinsic Triplet State Lifetime Fitting Procedure

When the intrinsic lifetime of triplet states is long and the concentration of the triplet states is high, the triplet-triplet annihilation will contribute additional lifetime quenching factor to the decay of the transient absorption. Then triplet state lifetime will be quenched significantly and the experimental values will be shorter than the intrinsic lifetime. The corresponding differential equations for the triplet concentration fitting of the decay traces are given below. We fitted the decay curves taken at different concentrations (c = 5.0 × 10^{-6} M and 2.0 × 10^{-5} M) with a kinetic model to eliminate the TTA self-quenching effect with equation S4.[4,5]

$$\frac{dc_T}{dt} = -k_1 c_T - k_2 {c_T}^2 \qquad \text{(S4)}$$

has the solution:

$$c_{\mathrm{T}}(t) = \frac{c_0\, k_1}{\exp(k_1 t) \cdot (c_0 k_2 + k_1) - c_0 k_2} \qquad \text{(S5)}$$

Where c_0 is the initial triplet concentration. This leads to the following expression for the triplet absorption

$$A(t) = \frac{A_0 \tau_2/\tau_1}{\exp(t/\tau_1) \cdot (1 + \tau_2/\tau_1) - 1} \qquad \text{(S6)}$$

Where $A(t)$ and A_0 are the optical density (Δ O.D.) values of the triplet state decay traces at t and 0 moment; τ_1 is the intrinsic triplet state lifetime; τ_2 is the triplet state lifetime related with TTA quenching effect. This kind of fitting was rarely used in the determination of the triplet state lifetimes by using ns-TA spectroscopy. As a result, some of the reported triplet states lifetimes are shorter than the 'real' triplet state lifetimes.

11. Femtosecond transient absorption spectroscopy

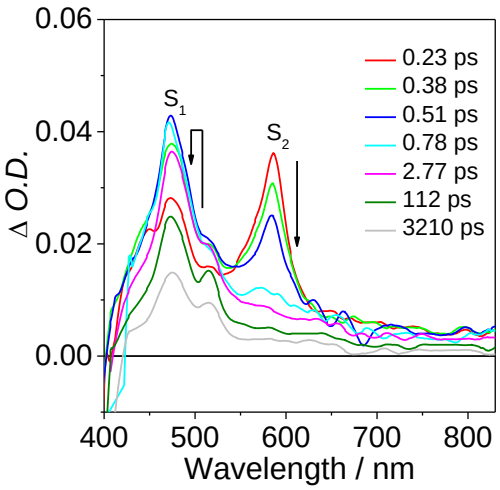

Figure S28. Femtosecond time-resolved transient absorption spectra of **Pyrene** at different time delays in DCM. λ_{ex} = 330 nm. 20 °C.

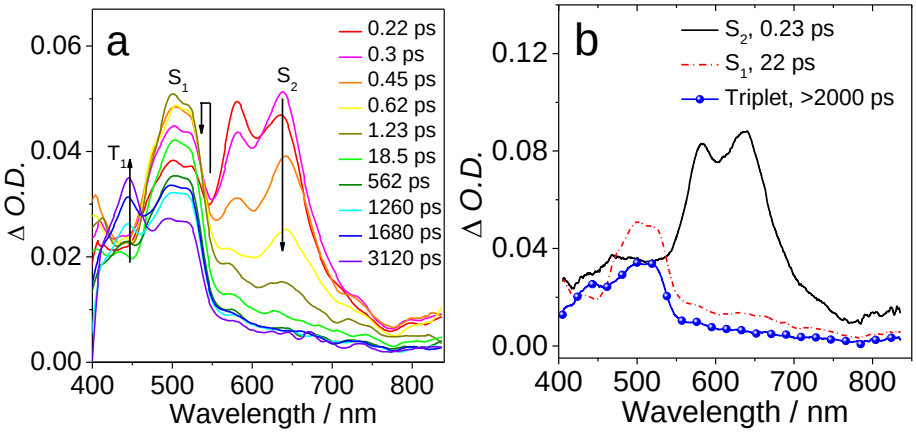

Figure S29. (a) Femtosecond time-resolved transient absorption spectra of **Py-Ph** at different time delays, (b) the evolution associated difference spectra (EADS) of **Py-Ph** obtained after globals analysis. In *n*-hexane. λ_{ex} = 340 nm. 20 °C.

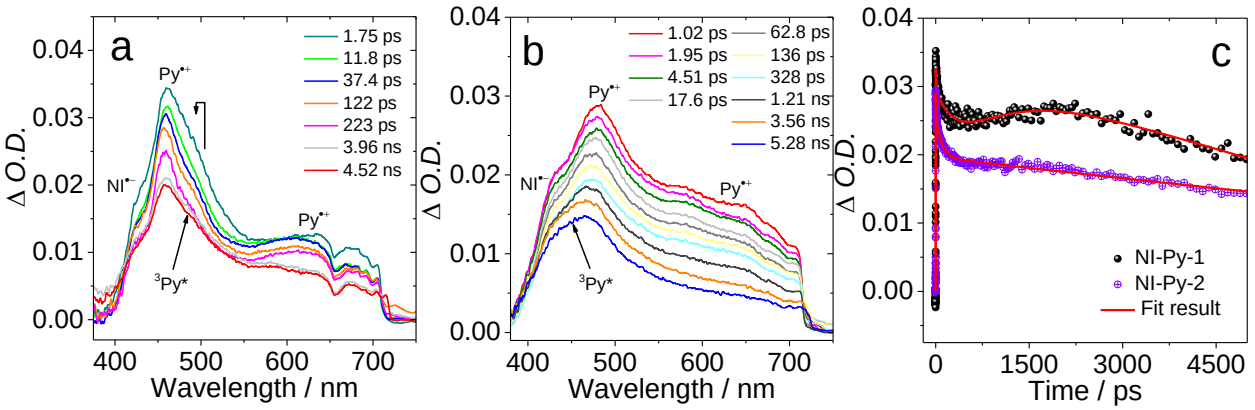

Figure S30. Femtosecond time-resolved transient absorption spectra of (a) **NI-Py-1,** (b) **NI-Py-2** at different time delays and (c) decay traces at 465 nm. In ACN. λ_{ex} = 350 nm. 20 °C.

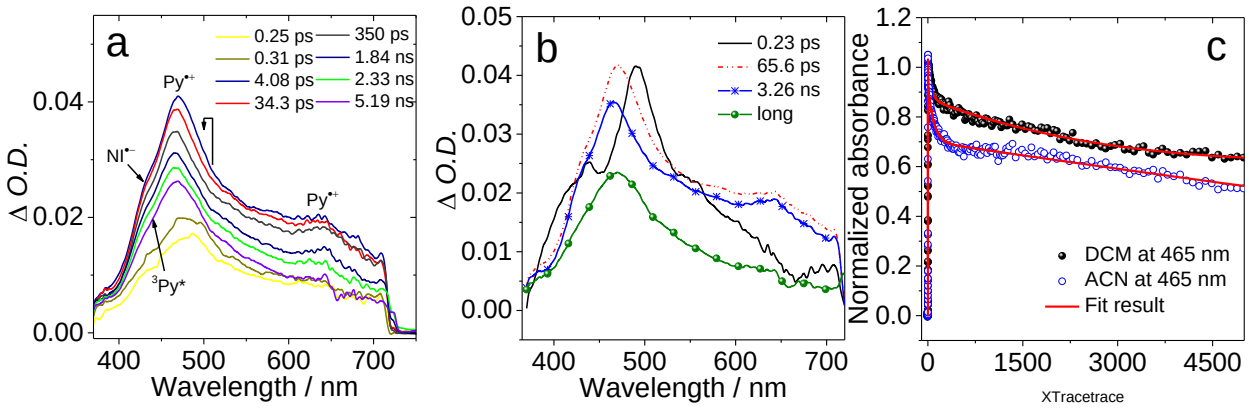

Figure S31. Femtosecond transient absorption spectra of (a) **NI-Py-2** at different time delays (b) the EADS obtained after global analysis and (c) decay traces at 465 in DCM and ACN. λ_{ex} = 350 nm. 20 °C.

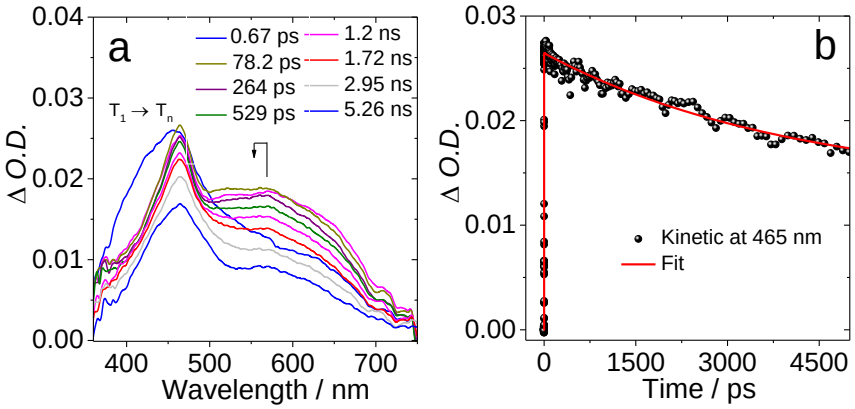

Figure S32. Femtosecond transient absorption spectra of (a) **NI-3Ph** at different time delays and (b) decay traces at 465 nm. In toluene. λ_{ex} = 350 nm. 20 °C.

12. Computational study

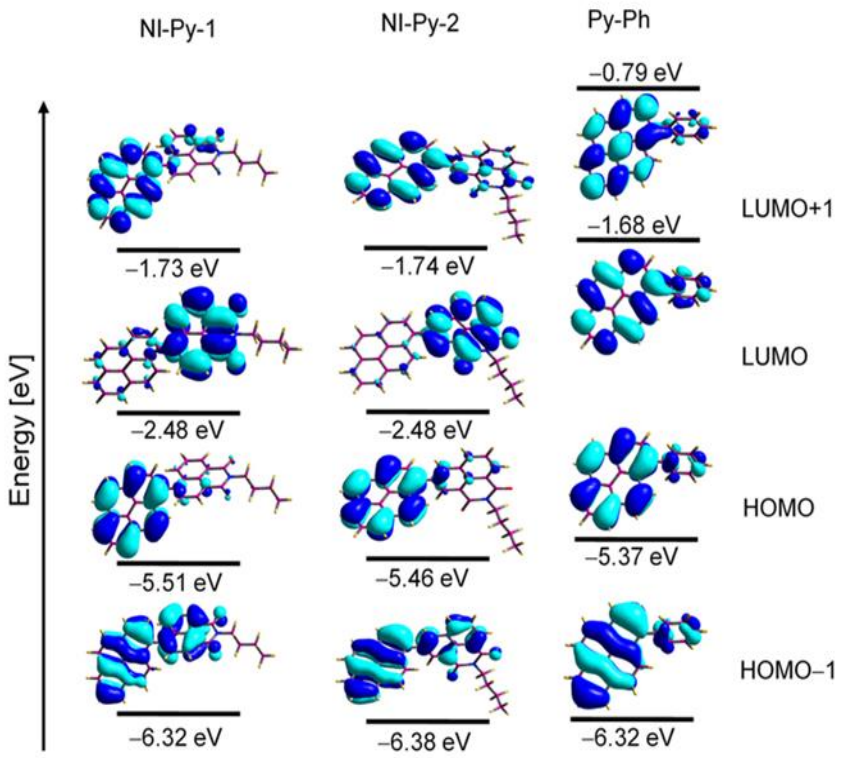

Figure S33. Frontier molecular orbitals of the compounds at optimized singlet ground state geometries (S_0) (isovalue is 0.02). The calculation was performed at B3LYP/6−31G (d) level using Gaussian 09W.

Scheme S1. Jablonski Diagram Indicating the Photophysical Processes Involved in (a) NI-3Ph in toluene and (b) NI-Py-2 in DCM, Upon Direct Photoexcitation [a]

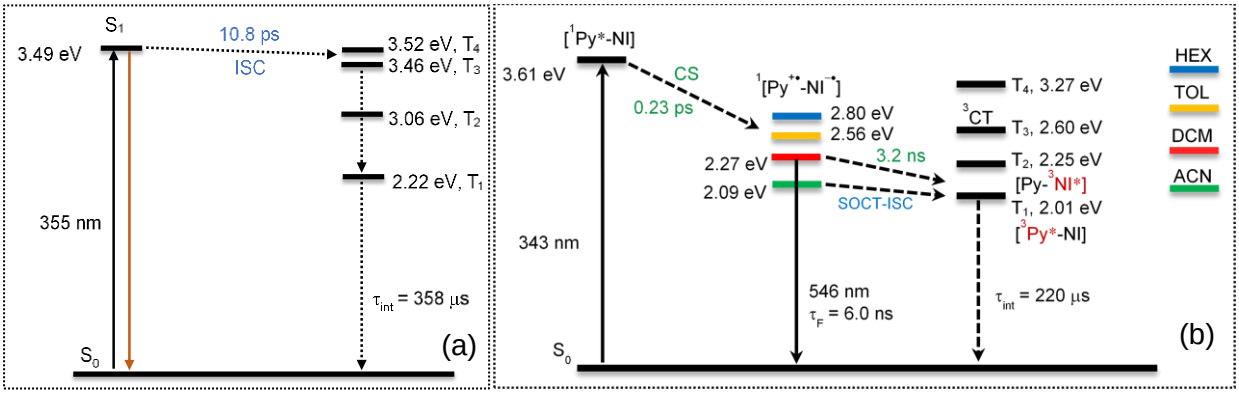

[a] The energy levels of the singlet excited states are derived from the spectroscopic data and CT states energy levels in different polarity solvents are obtained from the CT emission band. The triplet state energy levels are estimated by TD-DFT method. The numbers in superscripts indicate the spin multiplicity.

13. x,y,z coordinates of the optimized geometries

NI-Py-1

Charge = 0; Multiplicity = 1

Symbolic Z–Matrix:

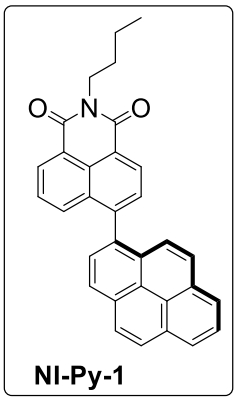

C 6.88715200	-0.95035100	0.25989200
C 5.94392600	-1.85252500	0.64784700
C 4.54548000	-1.52064400	0.63808300
C 3.55963600	-2.43895600	1.03062000
C 4.14307800	-0.21680000	0.21426700
C 2.75682000	0.14444900	0.20325500
C 1.79279100	-0.80786600	0.62134700
C 2.21509600	-2.08624000	1.01754700
C 0.33946800	-0.47657500	0.70110000
C -0.62467900	-1.13323400	-0.13508300
C -2.01224300	-0.82859000	0.03719300
C -2.41786300	0.11730800	1.01153900
C -1.46652400	0.75199200	1.79073200
C -0.10172400	0.45383400	1.63379400
C -0.26657700	-2.06127500	-1.15031900
C -1.22737400	-2.66835200	-1.93480300
C -2.59182800	-2.37647100	-1.74658300
C -2.98250800	-1.46830200	-0.77722000
C -3.85008000	0.43809300	1.20163500
C -4.42296500	-1.16747800	-0.60453700
N -4.76861600	-0.24913600	0.39623500
O -5.29370600	-1.69095500	-1.29454100
O -4.23906900	1.26307400	2.02424900
C -6.20111400	0.05260000	0.58259400

C	-6.68262600	1.20899500	-0.30036400
C	-8.17072000	1.51472000	-0.08862300
C	-8.67023000	2.66843500	-0.96430000
C	5.13504500	0.72563900	-0.19908100
C	4.74954000	2.02890100	-0.63729600
C	3.35165700	2.35565100	-0.65897500
C	2.40417700	1.46114800	-0.26168600
C	6.51937100	0.36839200	-0.17816800
C	7.47572100	1.31337500	-0.58585000
C	7.08834500	2.58419200	-1.00983000
C	5.74080700	2.94062700	-1.03750900
H	7.94137400	-1.21518200	0.27315700
H	6.23394600	-2.84784400	0.97468100
H	3.85557200	-3.43299100	1.35541400
H	1.47111300	-2.80861600	1.34122700
H	-1.78982500	1.47406800	2.53286700
H	0.62437100	0.94894900	2.27113300
H	0.78163900	-2.28859600	-1.30974800
H	-0.93085900	-3.37249900	-2.70596100
H	-3.35178500	-2.85058800	-2.35835700
H	-6.74992400	-0.86090200	0.35015800
H	-6.33850700	0.29343600	1.63749300
H	-6.08533200	2.10222100	-0.07689400
H	-6.50227900	0.95431200	-1.35252500
H	-8.76118400	0.61213500	-0.29977700
H	-8.34533000	1.75547200	0.96938200
H	-9.73476700	2.86507900	-0.79377200
H	-8.12059500	3.59337000	-0.75075300
H	-8.53804000	2.44193500	-2.02937100
H	3.05723400	3.34238900	-1.00760500
H	1.35618900	1.73759500	-0.29850500

H 8.52813100	1.04180400	-0.56798100
H 7.84238500	3.30140700	-1.32170700
H 5.44466400	3.93188900	-1.37117200

Calculation Type = FREQ

Calculation Method = RB3LYP

Basis Set = 6−31G(d)

Charge = 0

Spin = Singlet

E(RB3LYP) = −1438.594542 a.u.

RMS Gradient Norm = 0.000003 a.u.

Imaginary Freq = 0

Dipole Moment = 5.262473 Debye

Point Group = C1

NI-Py-2

Charge = 0; Multiplicity = 1

Symbolic Z−Matrix:

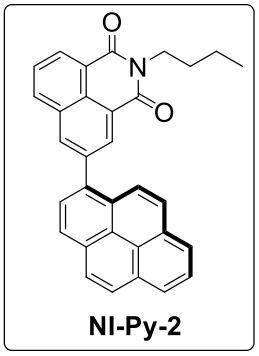

C 4.59453900	-1.31392700	-0.93056800
C 3.98303600	-0.24056700	-0.21173400
C 3.80169000	-2.40250800	-1.32369000
C 2.44168000	-2.42938400	-1.03860800
C 1.80832500	-1.38079800	-0.35398000
C 2.58200600	-0.27483900	0.08700100
C -2.19122100	-3.86925000	1.29686500
C -1.60850100	-2.73430300	0.67189700
C -2.46787300	-1.68683000	0.22570700
C -3.86830200	-1.79508600	0.40957000
C -4.40200600	-2.91604500	1.02431200
C -3.55870600	-3.95588500	1.46815000

C	-0.21014600	-2.59754600	0.47997900
C	0.33942600	-1.47381700	-0.12335400
C	-0.53570900	-0.44703300	-0.56608100
C	-1.90474400	-0.54632500	-0.39804800
C	-4.76428600	-0.70999700	-0.05186200
C	-2.78170900	0.54710800	-0.87938100
N	-4.16222200	0.38353700	-0.69323000
O	-2.34199000	1.55847100	-1.41884800
O	-5.98143000	-0.74564200	0.10486200
C	-5.04551600	1.46827800	-1.16473300
C	-5.27313000	2.54783200	-0.10130400
C	-6.19368200	3.66766100	-0.60299300
C	-6.42944200	4.75767400	0.44747800
C	4.78357800	0.86558400	0.21223400
C	4.19602600	1.93692000	0.95120700
C	2.79844500	1.85940900	1.26764200
C	2.03281600	0.80805300	0.86167100
C	5.99953700	-1.24817700	-1.22637200
C	6.75647200	-0.18750500	-0.83161300
C	6.17918500	0.90514300	-0.09741000
C	6.94292800	2.00586600	0.32522300
C	6.35742900	3.04888400	1.04246400
C	4.99947400	3.01667900	1.35526600
H	4.25768900	-3.22495500	-1.86858300
H	1.84283100	-3.27016900	-1.37695100
H	-1.54290800	-4.67108000	1.63979700
H	-5.47660700	-2.98028500	1.15757800
H	-3.99274500	-4.82787700	1.94735200
H	0.44323000	-3.39249800	0.82951900
H	-0.13749800	0.43109000	-1.06275900
H	-5.99099500	1.00535600	-1.44963600

H -4.57573300	1.89646800	-2.05106000
H -4.30345200	2.96920400	0.19304300
H -5.70828800	2.08271800	0.79249700
H -7.15797200	3.23701300	-0.90712200
H -5.75946400	4.11776000	-1.50675100
H -7.08696600	5.54525200	0.06228300
H -5.48487800	5.22736100	0.74801400
H -6.89630900	4.34339800	1.34942500
H 2.35558000	2.66097900	1.85347500
H 0.98528000	0.77567900	1.13962900
H 6.44800900	-2.07113800	-1.77711900
H 7.81782700	-0.15079500	-1.06389400
H 8.00306800	2.03601000	0.08679100
H 6.96473000	3.89142100	1.36120800
H 4.54876400	3.83007400	1.91815800

Calculation Type = FREQ

Calculation Method = RB3LYP

Basis Set = 6−31G(d)

Charge = 0

Spin = Singlet

E(RB3LYP) = −1438.592629 a.u.

RMS Gradient Norm = 0.000002 a.u.

Imaginary Freq = 0

Dipole Moment = 6.044402 Debye

Point Group = C1

14. References:

(1) Bandi, V.; Gobeze, H. B.; Lakshmi, V.; Ravikanth, M.; D'Souza, F. Vectorial Charge Separation and Selective Triplet-State Formation during Charge Recombination in a Pyrrolyl-Bridged BODIPY-Fullerene Dyad. *J. Phys. Chem. C* **2015**, 119, 8095−8102.

(2) Ziessel, R.; Allen, B. D.; Rewinska, D. B.; Harriman, A. Selective Triplet-State Formation During Charge Recombination in a Fullerene/Bodipy Molecular Dyad (Bodipy borondipyrromethene). *Chem. – Eur. J*. **2009**, 15, 7382−7393.

(3) Collini, M. A.; Thomas, M. B.; Bandi, V.; Karr, P. A.; D'Souza, F. Directly Attached Bisdonor BF2 Chelated Azadipyrromethene-Fullerene Tetrads for Promoting Ground and Excited State Charge Transfer. *Chem. – Eur. J*. **2017**, 23, 4450−4461.

(4) Lou, Z.; Hou, Y.; Chen, K.; Zhao, J.; Ji, S.; Zhong, F.; Dede, Y.; Dick, B. Different Quenching Effect of Intramolecular Rotation on the Singlet and Triplet Excited States of Bodipy. *J. Phys. Chem. C* **2018**, *122*, 185−193.

(5) Wang, Z.; Sukhanov, A. A.; Toffoletti, A.; Sadiq, F.; Zhao, J.; Barbon, A.; Voronkova, V. K.; Dick, B. Insights into the Efficient Intersystem Crossing of Bodipy-Anthracene Compact Dyads with Steady-State and Time-Resolved Optical/Magnetic Spectroscopies and Observation of the Delayed Fluorescence. *J. Phys. Chem. C* **2019**, *123*, 265−274.